Supplementary Material for "Much faster heat/mass than momentum transport in rotating Couette flows"

Geert Brethouwer*

Department of Engineering Mechanics,

KTH, SE-10044 Stockholm, Sweden

(Dated: December 23, 2020)

Abstract

Sec. S1. gives the schematic representations of the flow geometries and the equation of motion in cylindrical coordinates. Sec. S2. presents tables with the simulation parameters. Sec. S3. presents some validations of the DNSs.

S1. FLOW GEOMETRIES AND EQUATION OF MOTION IN CYLINDRICAL COORDINATES

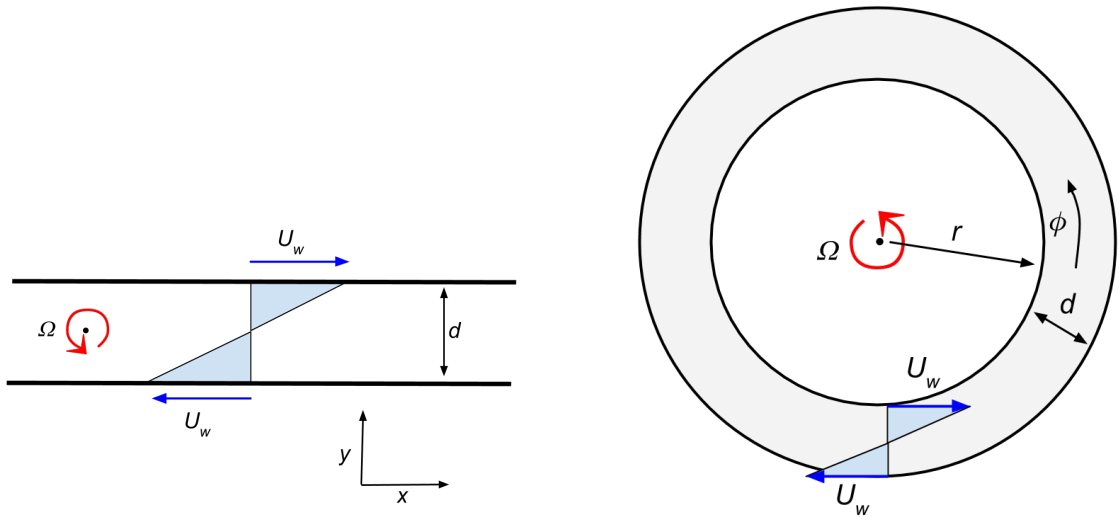

FIG. S1. Schematic representation of the PCF (left) and TCF system (right, seen from above), together with the coordinate systems and rotation axes. The streamwise and wall-normal (PCF), and radial and azimuthal directions (TCF) are in the plane of the paper. The rotation is about spanwise (PCF) and central (TCF) axes pointing out of the paper.

The non-dimensional equation of motion for TCF in cylindrical coordinates are given by [2, 3]

$$\frac{\partial \mathbf{U}}{\partial t} + (\mathbf{U}\cdot\widetilde{\nabla})\mathbf{U} = -\widetilde{\nabla}P + \frac{1}{Re}\widetilde{\Delta}\mathbf{U} - \underbrace{R_\Omega(\boldsymbol{e}_z \times \mathbf{U})}_{I} + \underbrace{R_C\frac{\tilde{r}}{r}\left[U^2\boldsymbol{e}_r - UV\boldsymbol{e}_\phi\right]}_{II}, \tag{1}$$

where

$$\widetilde{\nabla} = \boldsymbol{e}_r\partial_r + \boldsymbol{e}_\phi\frac{1}{r}\partial_\phi + \boldsymbol{e}_z\partial_z \tag{2}$$

$\widetilde{\Delta}$ is the modified Laplace operator [2], U and V the azimuthal and radial velocity components, respectively, and $(\boldsymbol{e}_r, \boldsymbol{e}_\phi, \boldsymbol{e}_z)$ the unit vectors in radial, azimuthal and axial direction, respectively. The last term II in equation (1) is owing to curvature. Here, $R_C = (1-\eta)/\sqrt{\eta}$ is the curvature number and $\tilde{r} = \sqrt{r_i r_o}$ a typical radius, see [3] and [2]. If we take the radius as $r = \tilde{r}$ we find that the ratio of the curvature term II and rotation term I in equation (1) is $R_C U/(2R_\Omega)$, where U is non-dimensionalized by U_w.

S2. SIMULATION PARAMETERS

Re	R_Ω															
240	0	0.125	0.25	0.5	0.7	0.8	0.85	0.9	0.93	0.97						
400	0	0.125	0.25	0.5	0.7	0.8	0.9	0.95	0.98	0.99						
800	0	0.125	0.25	0.5	0.7	0.8	0.9	0.95	0.98	0.99	1					
1600	-0.01	0	0.125	0.25	0.5	0.7	0.8	0.9	0.95	0.97	0.98	0.99	1			
3200	-0.02	0	0.125	0.25	0.5	0.7	0.8	0.9	0.95	0.97	0.98	0.99	1			
6400	-0.04	0	0.125	0.25	0.5	0.7	0.8	0.9	0.95	0.97	0.98	0.99	1			
17 200	-0.1	-0.08	-0.04	0	0.125	0.25	0.5	0.7	0.8	0.9	0.95	0.98	0.99	1		
40 000	-0.18	-0.15	-0.12	-0.1	-0.04	0	0.125	0.25	0.5	0.7	0.8	0.9	0.95	0.98	0.99	1

TABLE S1. Re and R_Ω of the DNS of rotating PCF.

Re	R_Ω											
400	-0.17	-0.06	0	0.09	0.17	0.29	0.36	0.46	0.58	0.74	0.85	0.89
	0.92	0.94	0.97	0.985	0.99							
1152	-0.17	-0.06	0	0.09	0.17	0.22	0.29	0.36	0.46	0.58	0.74	0.85
	0.92	0.94	0.97	0.985	1							
2593	-0.17	-0.06	0	0.09	0.17	0.22	0.29	0.36	0.46	0.58	0.74	0.85
	0.92	0.94	0.97	0.985	0.999	1.01						
3889	-0.17	-0.06	0	0.09	0.17	0.22	0.29	0.36	0.46	0.58	0.74	0.85
	0.92	0.94	0.97	0.985	0.999	1.01						
8750	-0.26	-0.22	-0.17	-0.06	0	0.09	0.17	0.29	0.36	0.46	0.58	0.74
	0.85	0.92	0.94	0.97	0.985	0.999	1.01					
19 688	-0.26	-0.17	-0.06	0	0.09	0.17	0.29	0.36	0.46	0.58	0.74	0.85
	0.92	0.94	0.97	0.985	0.999	1.01						
29 531	-0.17	-0.06	0	0.09	0.17	0.29	0.46	0.58	0.74	0.85	0.92	0.94
	0.97	0.985	0.991	0.996	0.999	1.01						
40 000	0	0.11	0.29	0.46	0.58	0.74	0.85	0.92	0.94	0.97	0.985	0.991

TABLE S2. Re and R_Ω of the DNS of rotating TCF.

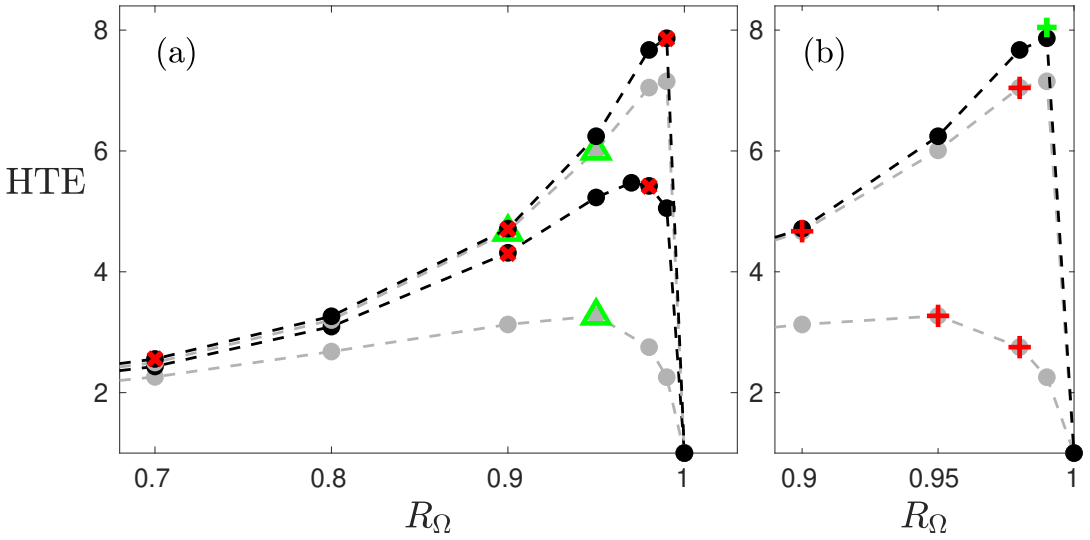

FIG. S2. HTE versus R_Ω for PCF. The gray and black filled circles are the original DNS data at $Re = 800$, 17 200 and $Re = 6400$, 40 000, respectively. The green triangles and red crosses in (a) are data of DNSs at higher resolutions. The red plus signs in (b) are data of DNSs with a larger domain size and the green plus sign in (b) data of a DNS with a much smaller domain size.

S3. VALIDATION OF THE SIMULATIONS

In order to validate the numerical approach I have performed several additional DNSs of PCF at a higher resolution. Fig. S2.a shows that the results of these DNSs overlap the results of the original DNSs. Furthermore, I have carried out two DNSs at $Re = 800$ with a four times larger domain size and two DNSs at $Re = 17\,200$ with a 2.5 times larger domain size. Also the results of these DNSs are the same as of the original ones, see Fig. S2.b. Finally, I have carried out a DNS at $(Re, R_\Omega) = (40\,000, 0.99)$ with a much smaller domain of πd long and $\pi d/4$ wide. The result of this DNS is almost identical to that of the original DNS, see Fig. S2.b. All these comparisons show that the resolutions and computational domain size are adequate.

To validate my DNSs of TCF I have compared results for Nu_m with previously reported DNS data. A useful and equivalent expression for the rotation number for TCF in this respect is

$$R_\Omega = \frac{1-\eta}{\eta}\,\frac{\eta - a}{1+a} \tag{3}$$

where $a = -\omega_o/\omega_i$ and ω_i and ω_o are the angular velocities of the inner and outer cylinders, respectively, in a laboratory frame of reference [4]. More relations between Re and R_Ω and

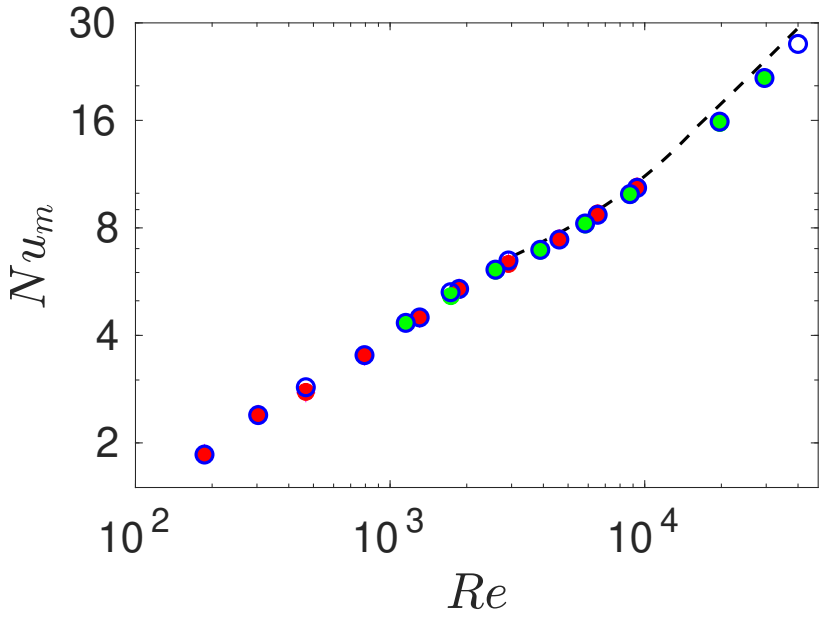

FIG. S3. Nu_m versus Re for $R_\Omega = 1 - \eta$. The open circles are my DNS data, the red and green dots are DNS data by [1, 6], respectively, and the dashed line is a fit to the experimental data of [5].

other much used non-dimensional numbers are given in e.g. [2, 3]. Fig. S3 shows my and DNS results by [1, 6] and a fit to experimental results by [5] for various Re for $R_\Omega = 1 - \eta$ corresponding to $a = 0$, i.e. the case with a non-rotating outer cylinder in the laboratory frame of reference. Fig. S4 shows data of my and DNS series by [1] at the same constant Re and varying a. Expression (3) is used to make the conversion from the rotating frame to the laboratory frame of reference to compute a. Results are shown for DNS series at $Re = 1152$ up to 29 531. Note that in addition to the DNSs reported in the main article I have carried out DNSs at other Re for validation. It can be seen that my results agree well with previous ones.

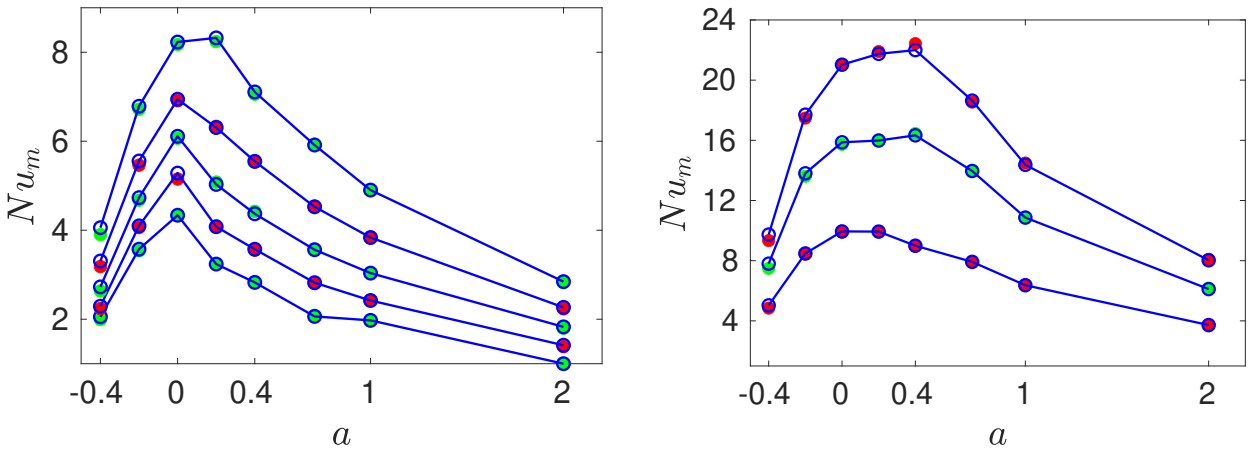

FIG. S4. Nu_m versus a. Each line represents a DNS series with constant Re. The open circles are my DNS data whereas the red and green dots are DNS data by [1]. The left plot shows results for Re from 1152 to 5833 and the right plot for Re from 8750 to 29 531.

* geert@mech.kth.se

[1] Brauckmann, H. J. & Eckhardt, B. 2013 Direct numerical simulations of local and global torque in Taylor-Couette flow up to $re = 30\,000$. *J. Fluid Mech.* **718**, 398–427.

[2] Brauckmann, H. J., Salewski, M. & Eckhardt, B. 2016 Momentum transport in Taylor-Couette flow with vanishing curvature. *J. Fluid Mech.* **790**, 419–452.

[3] Dubrulle, B., Dauchot, O., Daviaud, F., Longaretti, P.-Y., Richard, D. & Zahn, J.-P. 2005 Stability and turbulent transport in Taylor-Couette flow with analysis of experimental data. *Phys. Fluids* **17**, 095103.

[4] van Gils, D. P. M., Huisman, S. G., Bruggert, G.-W., Sun, C. & Lohse, D. 2011 Torque scaling in turbulent Taylor-Couette flow with co- and counterrotating cylinders. *Phys. Rev. Lett.* **106**, 024502.

[5] Lewis, G. S. & Swinney, H. L. 1999 Velocity structure functions, scaling, and transitions in high-Reynolds-number Couette-Taylor flow. *Phys. Rev. E* **59**, 5457–5467.

[6] Ostilla, R., Stevens, R. J. A. M., Grossmann, S., Verzicco, R. & Lohse, D. 2013 Optimal Taylor-Couette flow: direct numerical simulations. *J. Fluid Mech.* **719**, 14–46.